Supplementary Figure 1

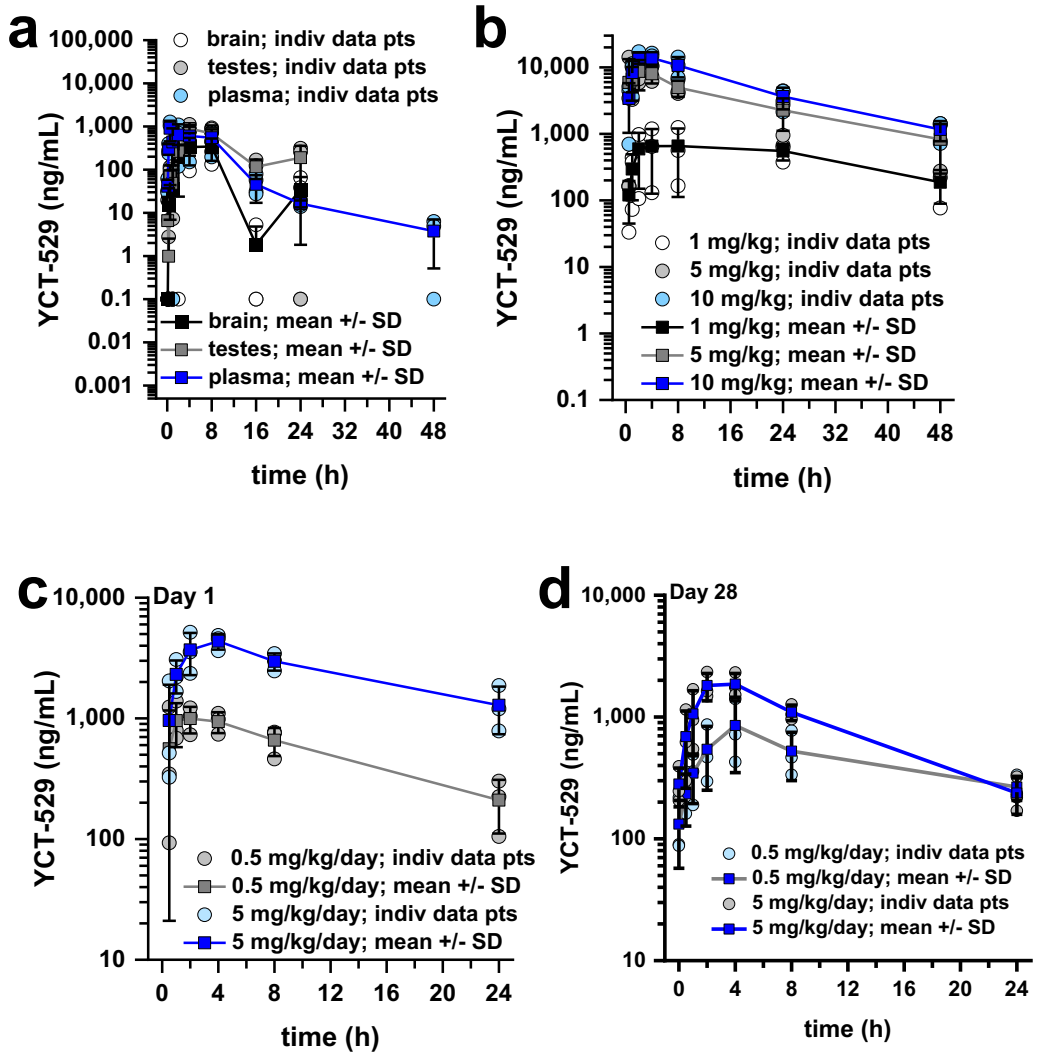

Supplementary Figure 1. Pharmacokinetics of YCT-529 in mice and NHPs. Mouse single dose administration (**a**): Thirty (30) CD-1 male mice (6-8 weeks, 30-35 g) were dosed orally by gavage with 10 mg/kg of **YCT-529** in saline. Shown are YCT-529 concentrations as individual data points in brain (white circles), testes (light grey circles), and plasma (light blue circles) from 3 animals per time point, respectively. Average concentrations ± S.D. in brain, testes, and plasma are depicted by the black, dark grey, and dark blue lines and squares, respectively. NHP single dose administration (**b**): Three (3) male non-naïve Cynomolgus macaques received a single oral dose of 1 (black), 5 (red), and 10 (blue) mg/kg/day of **YCT-529**. The doses were escalated after a 7-day washout period. Blood was collected at the indicated time points to assess **YCT-529** concentrations with LC-MS/MS. Shown are YCT-529 concentrations over 48 h as individual data points at 1 mg/kg (white circles), 5 mg/kg (light grey circles), and 10 mg/kg (light blue circles) from 3 animals per time point, respectively. Average concentrations ± S.D. at 1, 5, or 10 mg/kg are depicted by the black, dark grey, and dark blue lines and squares, respectively. NHP 28-Day repeat dose administration (**c** and **d**): Three (3) non-naïve Cynomolgus macaques per dose group received oral doses of **YCT-529** at 0.5 or 5 mg/kg/day. Blood was collected on Day 1 (**c**) and Day 28 (**d**) to assess 24-hour PK profiles. **YCT-529** concentrations were evaluated with LC-MS/MS. Shown are YCT-529 concentrations over 24 h as individual data points at 1 mg/kg (light grey circles) or 5 mg/kg (light blue circles) from 3 animals per time point, respectively. Average concentrations ± S.D. at 0.5 or 5 mg/kg are depicted by the dark grey and dark blue lines and squares, respectively.

Supplementary Figure 2

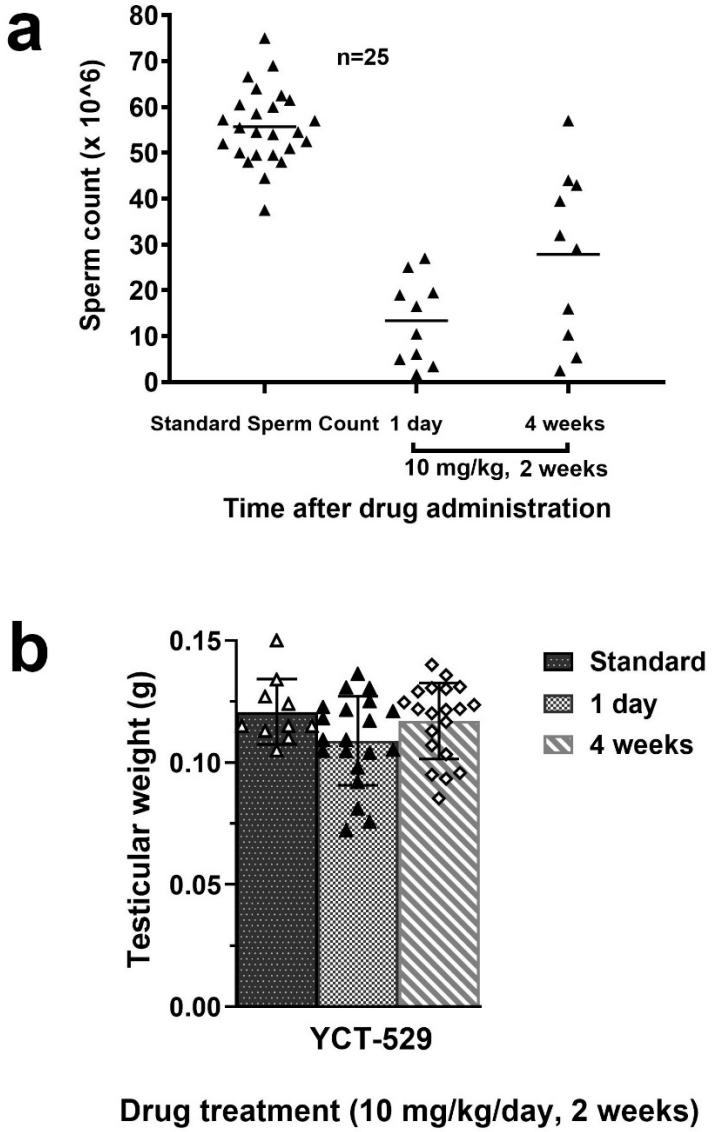

Supplementary Figure 2. Testicular and cauda epididymal sperm counts in mice treated with 10 mg/kg/day for 2 weeks. **a:** The cauda epididymal sperm counts of male mice at one day and 4-weeks post-CDT. The horizontal bars show the average number of sperm counts obtained at the assessed time point. **b**: The testicular weight of **YCT-529**-treated male mice at one day and 4 weeks post-CDT. The bars represent the mean ± SD of five mice for each time point; no significant difference was observed by 2-sided paired Student's t-test.

Supplementary Figure 3

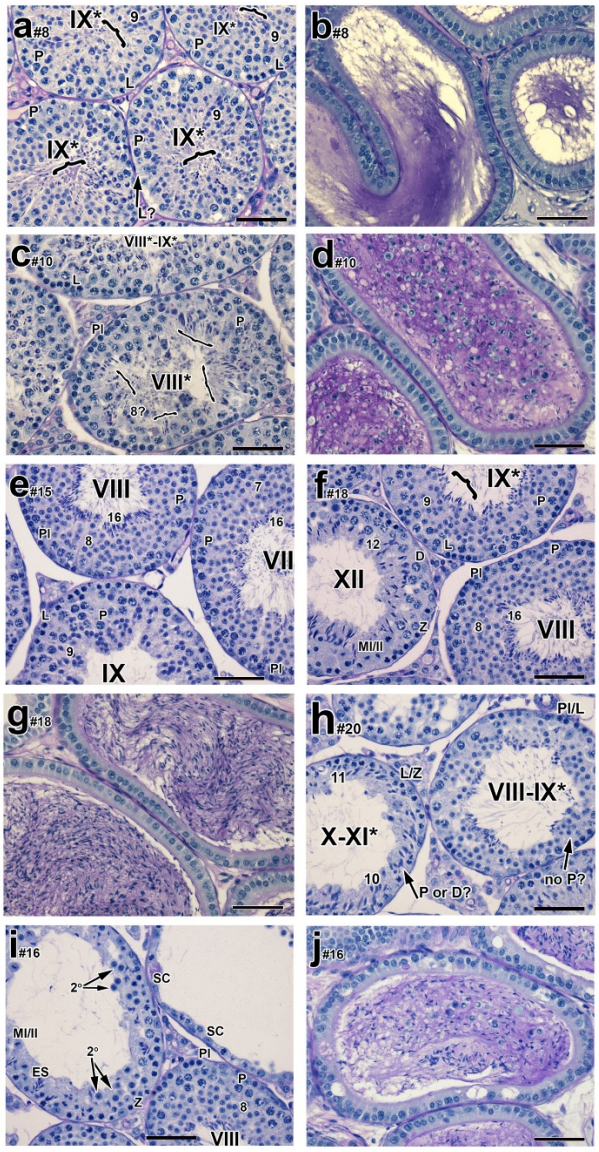

Supplementary Figure 3. More severe disruption of spermatogenesis in two YCT-529-treated males one day post-CDT while proper spermatid translocation but a failure of sperm release was found in most YCT-529-treated testes at 4 weeks post-CDT. a–d: Histological testicular and epididymal sections of male mice treated with 10 mg/kg/day of **YCT-529** for 2 weeks and terminated one day post-CDT. The two males with the most noticeably reduced testicular weight and sperm counts also exhibited a more severe disruption of testicular tubule morphology (**a** and **c**) and a reduced number or a lack of epididymal sperm (**b** and **d**). **e–j:** Histological testicular and epididymal sections of male mice treated with 10 mg/kg/day of **YCT-529** for 2 weeks and terminated 4 weeks post-CDT. Two of the infertile males with reduced testicular weight and sperm counts displayed more severely disrupted testicular morphology at 4 weeks post-CDT (**h** and **i**) and reduced numbers of epididymal sperm (**j**). Pl, preleptotene spermatocytes; L, leptotene spermatocytes; P, pachytene spermatocytes. Brackets in stage IX* tubules indicate retained spermatids. Arabic numerals indicate the step of spermatid differentiation. Roman numerals indicate the stage of the tubules. The drug-treated tubules are labeled with a Roman numeral followed by an asterisk (e.g., stage IX*). Scale bar in a-j, 50 μm.

Supplementary Figure 4

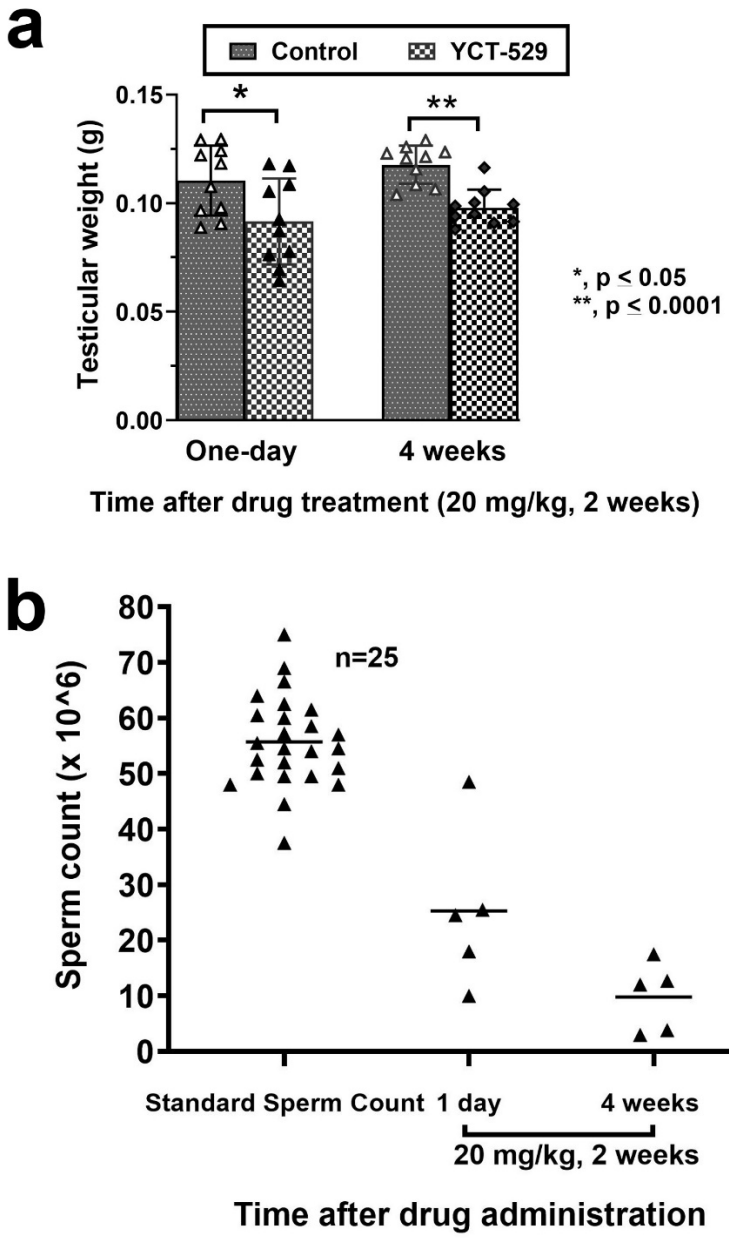

Supplementary Figure 4. Gonad weight and cauda epididymal sperm count in mice treated with 20 mg/kg/day for 2 weeks. **a:** The testicular weight of **YCT-529**-treated male mice at one day and 4-weeks post-CDT. At 4 weeks post-CDT, both a significant drop in testicular weight (0.10 g ± 0.01 versus standard control, 0.12g ± 0.01) and reduced sperm counts ($9.79 \times 10^6 \pm 6.23$ versus control $55.5 \times 10^6 \pm 8.18$, n=5) were still observed. The bars represent the mean ± SD of five mice for each time point. *, Significant differences within the same age group as assessed by 2-sideded paired Student's t-test. *, $P \leq 0.05$; **, $P \leq 0.0001$. **b:** The cauda epididymal sperm counts of compound-treated male mice at one day and 4-week post-CDT time points. The horizontal bars show the average number of sperm counts obtained at the assessed time point.

Supplementary Figure 5

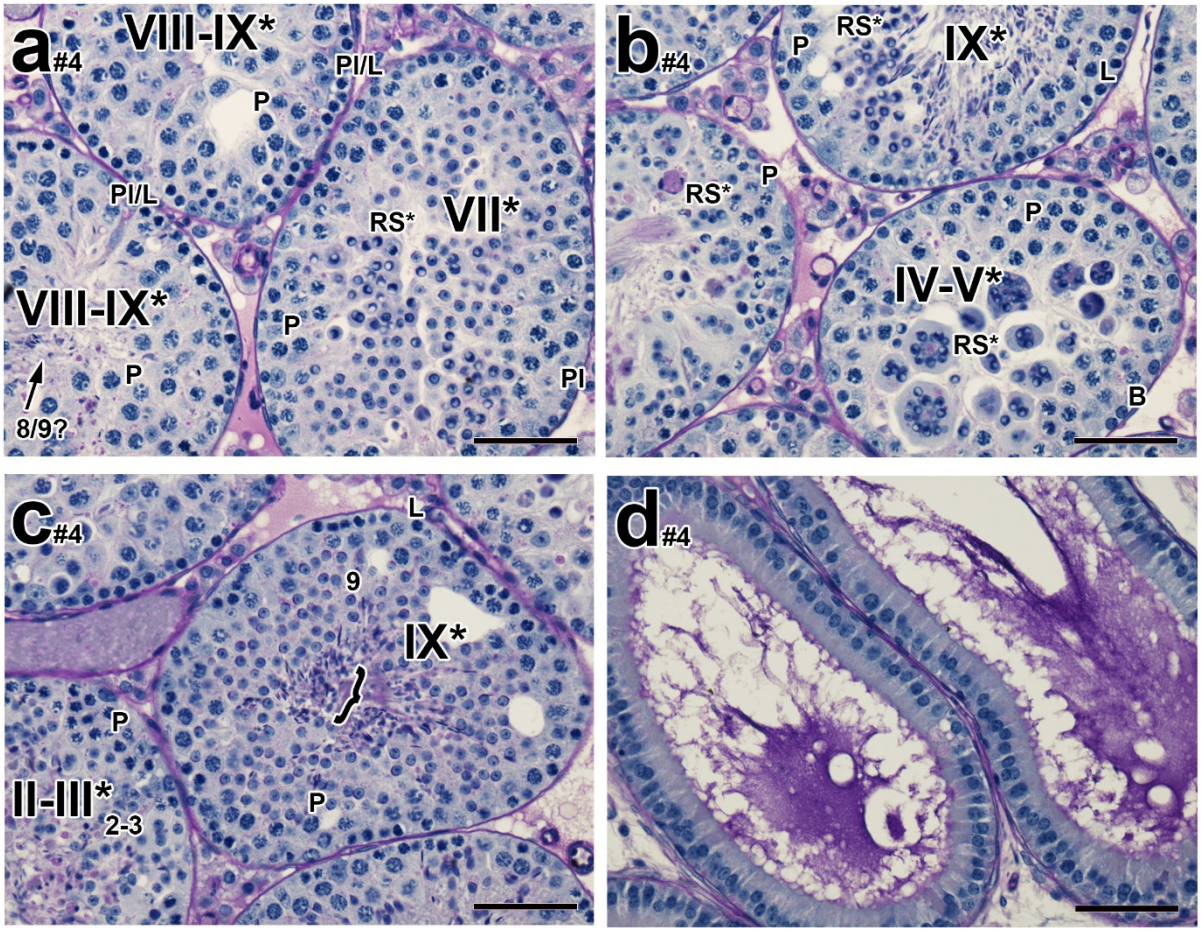

Supplementary Figure 5. More severe disruption of spermatogenesis in three males after a higher dose of YCT-529. a–d: Histological testicular and epididymal sections of male mice treated with 20 mg/kg/day of **YCT-529** for 2 weeks and terminated one day post-CDT. **a** and **b**: Either pachytene spermatocytes or round spermatids as the most advanced germ cells. **c** and **d**: spermatids that failed to translocate, and a lack of sperm in the corpus and caput epididymides. PI, preleptotene spermatocytes; L, leptotene spermatocytes; P, pachytene spermatocytes; RS, round spermatids; B, type B spermatogonia. Brackets in stage IX* tubules indicate retained spermatids. Arabic numerals indicate the step of spermatid differentiation. Roman numerals indicate the stage of the tubules. The drug-treated tubules are labeled with a Roman numeral followed by an asterisk (e.g., stage IX*). Scale bar in a-d, 50 μm.

Supplementary Figure 6

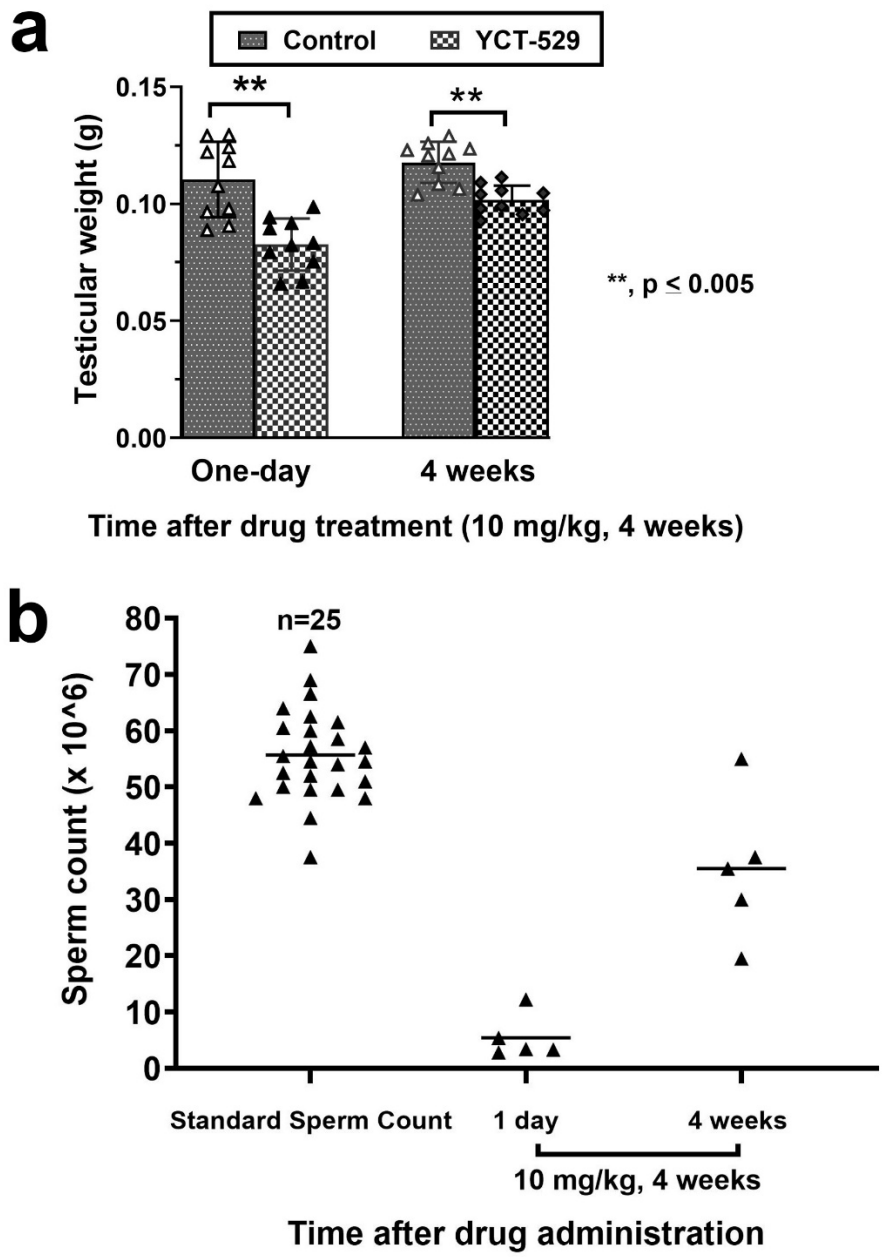

Supplementary Figure 6. Gonad weight and cauda epididymal sperm count in mice treated with 10 mg/kg/day for 4 weeks. **a:** The testicular weight of **YCT-529**-treated male mice at one day and 4 weeks post-CDT. The bars represent the mean ± SD of five mice for each time point. Significant differences within the same age group as assessed by 2-sided paired Student's t-test. **, P ≤ 0.005. **b**: Cauda epididymal sperm counts of compound-treated male mice at one day and 4 weeks post-CDT. The horizontal bars show the average number of sperm counts.

Supplementary Figure 7

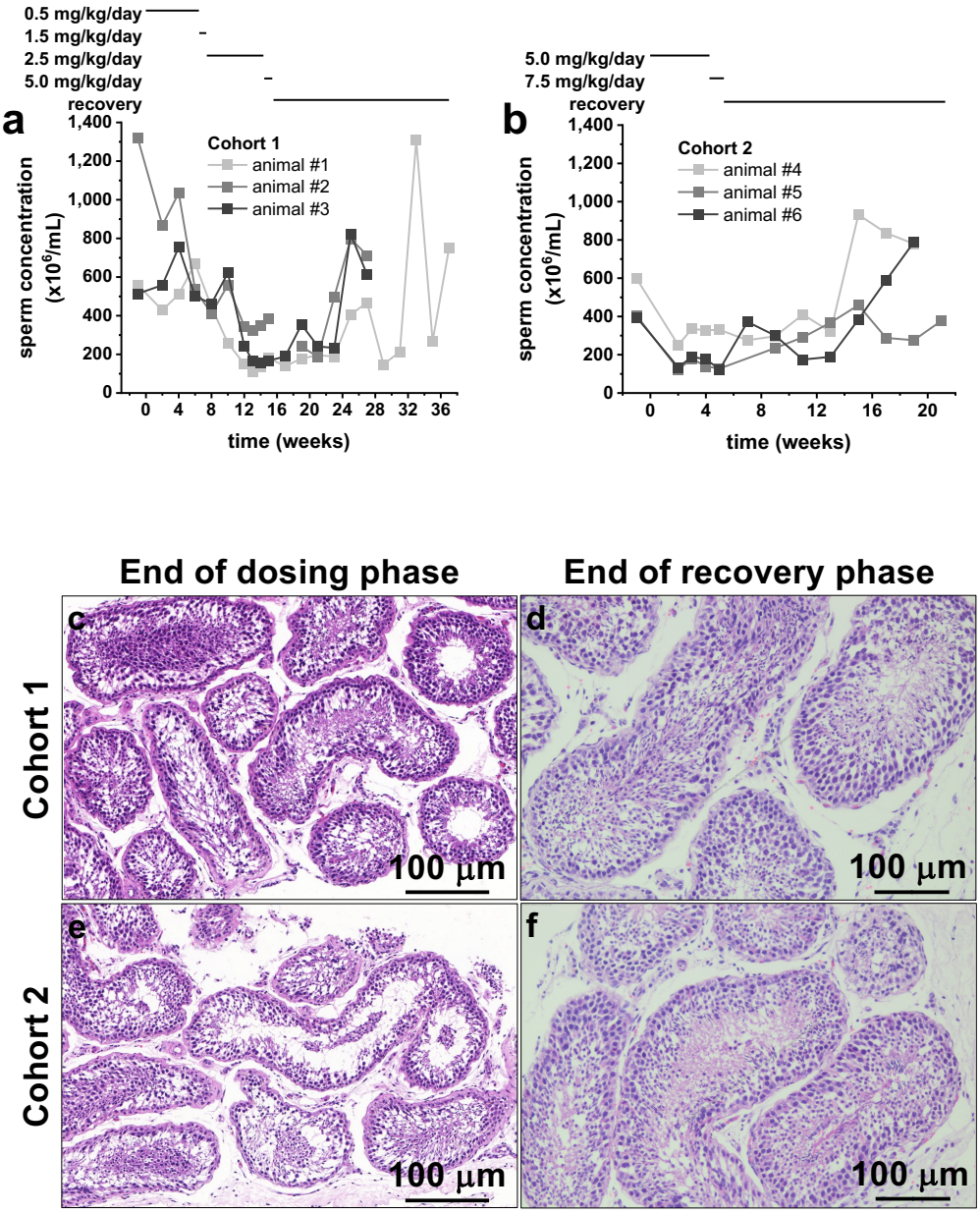

Supplementary Figure 7: Decrease and recovery of sperm concentrations and spermatogenesis in Cynomolgus monkeys. Three (3) sexually mature male animals were dosed per cohort. Fresh semen samples were obtained via electroejaculation at indicated time points. Cohort 1 (n=3) was dosed at 0.5 mg/kg/day (Day 1-46) followed by 1.5 mg/kg/day (Day 47-51), 2.5 mg/kg/day (Day 52-101) and 5 mg/kg/day (Day 102-108); the recovery phase was from Day 109 to Day 257. Cohort 2 (n=3) was dosed at 5 mg/kg/day (Day 1-30), followed by 7.5 mg/kg/day (Day 31-37); the recovery phase was from Day 38 to Day 145. Shown are individual sperm concentrations in millions/mL (light grey, dark grey, and black lines and squares) of all Cohort 1 (**a**) and Cohort 2 (**b**) animals. Testicular biopsies were taken from all 6 animals (one per left and right testis per animal) 24 h post-CDT (end of dosing phase; **c** and **e**), as well as 78 and 148 days (Cohort 1), and 93 and 107 days (Cohort 2) post-CDT (end of recovery phase; **d** and **f**). Shown are representative images.

Supplementary Table 1. Relevant PK parameters in mouse and NHP

Mouse PK parameters (single 10 mg/kg dose)			
	Blood plasma (n=2-3)	**Testis** (n=1-3)	**Brain** (n=1-3)
	Means		
C_{max} (ng/mL or ng/g)	907	900	343
T_{max} (h)	0.5	4.0	8.0
$T_{1/2}$ (h)	6.1	NC	NC
$AUC_{0\text{-}inf}$ (h*ng/ml)	7,713	NC	

NHP PK parameters (single dose)			
	1 mg/kg (n=3)	**5 mg/kg** (n=3)	**10 mg/kg** (n=3)
	Means ± S.D.		
C_{max} (ng/mL)	870 ± 324	9,416 ± 4,157	14,828 ± 2,301
T_{max} (h)	11.3 ± 11.4	2.2 ± 1.8	2.7 ± 1.2
$T_{1/2}$ (h)	40.5 ± 36.2	19.9 ± 1.3	18.7 ± 0.8
$AUC_{0\text{-}inf}$ (h*ng/mL)	33,394 ± 12,026	175,202 ± 64,119	293,423 ± 84,764

NHP dose proportionality (single dose)					
Compared doses (mg/kg/day)	**Dose ratio**	**C_{max} values (ng/mL)**	**C_{max} ratio**	**$AUC_{0\text{-}168h}$ values (h*ng/mL)**	**$AUC_{0\text{-}168h}$ ratio**
10 over 5	2	14,828/9,416	1.6	292,491/173,647	1.7
5 over 1	5	9,416/870	10.8	173,647/29,082	6.0
10 over 1	10	14,828/870	17.0	292,491/29,082	10.1

NHP PK parameters (repeat dose)			
	Day	**0.5 mg/kg/day** (n=3)	**5 mg/kg/day** (n=3)
		Means ± S.D.	
C_{max} (ng/mL)	1	1,076 ± 327	4,457 ± 776
	28	865 ± 487	2,097 ± 404
T_{max} (h)	1	1.5 ± 0.9	3.3 ± 1.2
	28	3.3 ± 1.2	2.7 ± 1.2
$T_{1/2}$ (h)	1	35.7 ± 26.4	36.0 ± 10.3
	28	36.8 ± 5.9	21.0 ± 9.3
$AUC_{0\text{-}48}$ (h*ng/mL)	1	9,100 ± 2,508	93,142 ± 23,877
	28	17,236 ± 6,945	29,085 ± 1,980

NHP dose proportionality (repeat dose)						
Compared doses (mg/kg/day)	**Dose ratio**	**Day**	**C_{max} values (ng/mL)**	**C_{max} ratio**	**$AUC_{0\text{-}168h}$ values (ng*h/mL)**	**$AUC_{0\text{-}168h}$ ratio**
5 over 0.5	10	1	4,457/1,076	4.1	93,142/9,100	10.2
		28	2,097/865	2.4	29,085/17,236	1.7

NHP PK parameters in blood plasma and seminal fluid (repeat dosing and recovery)								
	Cohort 1 (n=3)				**Cohort 2** (n=3)			
	Blood plasma		**Seminal fluid**		**Blood plasma**		**Seminal fluid**	
	EoD (Mean±S.D.)	**EoR**	**Day 28**	**EoR**	**EoD (Mean±S.D.)**	**EoR**	**Day 28**	**EoR**
Conc. (ng/mL)	298 ± 137	BQL	BQL	BQL	694 ± 404	BQL	BQL	BQL

AUC = area under the curve; C_{max} = peak plasma concentration; BQL = below quantification limit (20 ng/mL; <0.04 μM); EoD = end of dosing; EoR = end of recovery; NC = not calculated (concentration at the latter timepoint was higher than concentration at the previous timepoint); S.D. = standard deviation; $T_{1/2}$ = elimination half-life; T_{max} = time at which C_{max} is observed

Chemical synthesis of YCT-529.
Supplementary Figure 8 depicts the chemical synthesis of YCT-529, which is explained in greater detail below.

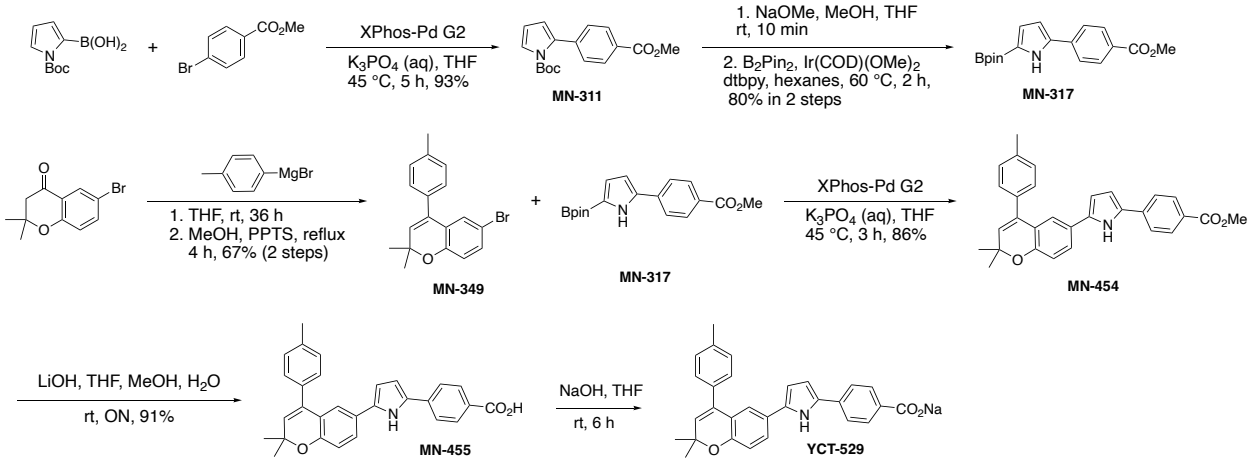

Supplementary Figure 8. Synthetic pathway for **YCT-529** synthesis.

***tert*-Butyl 2-(4-(Methoxycarbonyl)phenyl)-1*H*-pyrrole-1-carboxylate (MN-311).** Methyl 4-bromobenzoate (17.00 g, 79.05 mmol, 1.0 equiv) and (1-(*tert*-butoxycarbonyl)-1*H*-pyrrol-2-yl)boronic acid (20.00 g, 94.78 mmol, 1.2 equiv), were combined in a round bottom flask followed by addition of THF (190 mL) and an aqueous solution of potassium phosphate tribasic (0.5 M, 380 mL, 2.4 equiv). Nitrogen gas was bubbled through the reaction mixture for 15 min followed by addition of XPhos Pd G2 (1.50 g, 1.91 mmol, 0.024 equiv). Then, the flask was placed into a preheated oil bath at 45 °C and stirred for 5 h. After the reaction was complete, brine was added, and the mixture was extracted with EtOAc (50 mL × 3) and dried over $MgSO_4$. The solvent was evaporated to dryness under reduced pressure. The residue was purified by flash column chromatography (silica gel, 100% hexanes to 20% EtOAc in hexanes) to obtain **MN-311** as a white solid (22.142 g, 93%): mp 72-74 °C; ^{1}H NMR (400 MHz, $CDCl_3$) δ 8.06 – 7.98 (m, 2H), 7.45 – 7.35 (m, 3H), 6.29 – 6.21 (m, 2H), 3.93 (s, 3H), 1.37 (s, 9H). ^{13}C NMR (100 MHz, $CDCl_3$) δ 167.1, 149.3, 139.1, 134.1, 129.1, 128.7, 123.6, 115.6, 111.0, 84.2, 52.2, 27.8.

Methyl 4-(5-(4,4,5,5-Tetramethyl-1,3,2-dioxaborolan-2-yl)-1*H*-pyrrol-2-yl)benzoate (MN-317). *tert*-Butyl 2-(4-(methoxycarbonyl)phenyl)-1*H*-pyrrole-1-carboxylate (**MN-311**) (18.13 g, 60.16 mmol, 1.0 equiv) was dissolved in THF (60 mL), and sodium methoxide (80 mL, 25 wt.% in MeOH, 6 equiv) was added. The mixture was stirred for 10 min and quenched with a saturated ammonium chloride solution. The resulting mixture was extracted with dichloromethane (50 mL × 3) and the organic phase was dried over $MgSO_4$ and evaporated under reduced pressure to dryness to provide the deprotected product as a white solid (11.615 g, 96%): mp 163-165 °C; ^{1}H NMR (400 MHz, $CDCl_3$) δ 8.62 (s, 1H), 8.09 – 8.01 (m, 2H), 7.59 – 7.51 (m, 2H), 6.95 (td, *J* = 2.7, 1.4 Hz, 1H), 6.69 (ddd, *J* = 3.8, 2.7, 1.4 Hz, 1H), 6.36 (dt, *J* = 3.7, 2.6 Hz, 1H), 3.94 (s, 3H). ^{13}C NMR (101 MHz, $CDCl_3$) δ 166.9, 136.8, 131.0, 130.4, 127.3, 123.1, 120.3, 110.7, 108.0, 52.1.

The product from the last step (12.00 g, 59.63 mmol, 1.0 equiv), bis(pinacolato)diboron (8.304 g, 32.7 mmol, 0.6 equiv), cyclooctadiene)(methoxy)iridium(I) dimer (0.60 g, 0.91 mmol, 0.02 equiv), and 4,4′-di-tert-butyl-2,2′-dipyridyl (0.484 g, 1.80 mmol, 0.03 equiv) were combined in a round bottom flask, evacuated under reduced pressure, and purged with nitrogen. This process was repeated three times, followed by adding hexanes (120 mL). The suspension was

refluxed under nitrogen for 2 h. After 2 h, the reaction mixture was solubilized in DCM. A silica gel slurry was prepared for subsequent flash column chromatography (silica gel, 100% hexanes to 20% EtOAc in hexanes) to obtain the pyrrole boronate product **MN-317** as an off-white solid (16.71 g, 86%): mp 149-151 °C; ^{1}H NMR (400 MHz, $CDCl_3$) δ 8.99 (s, 1H), 8.07 – 8.00 (m, 2H), 7.63 – 7.56 (m, 2H), 6.89 (dd, *J* = 3.7, 2.4 Hz, 1H), 6.69 (dd, *J* = 3.7, 2.5 Hz, 1H), 3.92 (s, 3H), 1.34 (s, 12H).^{13}C NMR (101 MHz, $CDCl_3$) δ 167.0, 136.4, 135.6, 130.5, 128.2, 124.0, 122.1, 109.3, 84.1, 52.2, 24.9.

6-Bromo-2,2-dimethyl-4-(*p*-tolyl)-2*H*-chromene (MN-349). To a solution of 6-bromo-2,2-dimethylchroman-4-one (8.00 g, 31.4 mmol, 1.0 equiv) in THF (20 mL), *p*-tolylmagnesium bromide (100 mL 1M in THF, 3.2 equiv) was added slowly over 15 min at 0 °C. The reaction mixture was slowly warmed to room temperature and stirred for 36 h. Then the reaction was quenched with saturated ammonium chloride solution at 0 °C and extracted with EtOAc (40 × 3 mL). The organic layers were collected, washed with brine, dried over $MgSO_4$, and evaporated under reduced pressure to obtain a semisolid crude product that was dissolved in anhydrous MeOH (60 mL). Pyridinium-*p*-toluenesulfonate (1.60 g, 6.37 mmol, 0.2 equiv) was added and the reaction mixture was refluxed for 4 h. Then the solvent was evaporated under reduced pressure, and the residue was dissolved in EtOAc : water (30 mL: 30 mL) and extracted with EtOAc (30 × 3 mL). The organic layer was washed with brine, dried over $MgSO_4$, and evaporated under reduced pressure. The residue was purified by flash column chromatography (silica gel, 100% hexanes to 5% EtOAc in hexanes) to obtain **MN-349** (6.89 mg, 67%) as a colorless liquid; ^{1}H NMR (400 MHz, $CDCl_3$) δ 7.30 – 7.27 (m, 1H), 7.25 (s, 4H), 7.16 (d, *J* = 2.4 Hz, 1H), 6.80 (d, *J* = 8.5 Hz, 1H), 5.65 (s, 1H), 2.44 (s, 3H) 1.51 (s, 6H). ^{13}C NMR (101 MHz, $CDCl_3$) δ 152.6, 137.9, 134.8, 134.0, 131.8, 129.9, 129.4, 128.6, 128.2, 124.6, 118.8, 112.9, 76.3, 27.7, 21.4.

Methyl 4-(5-(2,2-Dimethyl-4-(*p*-tolyl)-2*H*-chromen-6-yl)-1*H*-pyrrol-2-yl)benzoate (MN-454). 6-Bromo-2,2-dimethyl-4-(*p*-tolyl)-2*H*-chromene (**MN-349**) (580 mg, 1.76 mmol, 1.0 equiv) and methyl 4-(5-(4,4,5,5-tetramethyl-1,3,2-dioxaborolan-2-yl)-1*H*-pyrrol-2-yl)benzoate (**MN-317**) (630 mg, 1.93 mmol, 1.1 equiv) were dissolved in THF (3.5 mL) and then an aqueous solution of potassium phosphate tribasic (7 mL 0.5 M, 2.0 equiv) was added to the solution. N_2 was bubbled through the reaction mixture for 15 min, followed by adding XPhos Pd G2 (0.035 g, 0.04 mmol, 0.025 equiv). Then, the reaction mixture was placed in a preheated oil bath at 45 °C and stirred for 3 h. After the reaction was complete, brine was added to the reaction mixture, extracted with EtOAc (50 mL × 3), and dried over $MgSO_4$. The solvent was evaporated under reduced pressure and the residue was purified by flash column chromatography (silica gel, 100% hexanes to 20% EtOAc in hexanes) to obtain **MN-454** as a bright yellow solid (681 mg, 86%): mp 189-191 °C; Remaining metal catalysts were scavenged to levels <10 ppm. ^{1}H NMR (400 MHz, $CDCl_3$) δ 8.48 (s, 1H), 8.04 – 7.96 (m, 2H), 7.53 – 7.46 (m, 2H), 7.35 (dd, *J* = 8.3, 2.3 Hz, 1H), 7.29 (d, *J* = 8.2 Hz, 2H), 7.25 – 7.19 (m, 3H), 6.93 (d, *J* = 8.3 Hz, 1H), 6.64 (dd, *J* = 3.7, 2.6 Hz, 1H), 6.38 (dd, *J* = 3.7, 2.5 Hz, 1H), 5.66 (s, 1H), 3.91 (s, 3H), 2.42 (s, 3H), 1.51 (s, 6H). ^{13}C NMR (101 MHz, $CDCl_3$) δ 167.0, 152.9, 137.9, 136.7, 135.3, 135.0, 134.5, 131.3, 130.5, 129.7, 129.4, 128.7, 127.2, 125.4, 125.1, 123.1, 123.0, 121.8, 117.6, 109.9, 107.7, 76.2, 52.2, 27.7, 21.4.

4-(5-(2,2-Dimethyl-4-(*p*-tolyl)-2*H*-chromen-6-yl)-1*H*-pyrrol-2-yl)benzoic Acid (MN-455). To a solution of methyl 4-(5-(2,2-dimethyl-4-(*p*-tolyl)-2*H*-chromen-6-yl)-1*H*-pyrrol-2-yl)benzoate (**MN-454**) (600 mg, 1.33 mmol, 1.0 equiv) in THF (10 mL) and MeOH (10 mL), was added lithium

hydroxide (280 mg, 6.67 mmol, 5 equiv) dissolved in water (10 mL) and the resulting mixture was stirred for 20 h at room temperature. The organic solvents were evaporated under reduced pressure, and the aqueous suspension was acidified with 2N HCl to reach pH 1.0. Then, the reaction mixture was extracted with EtOAc (10 mL × 3), washed with brine, and dried over $MgSO_4$. The extract was purified by flash column chromatography (silica gel, 100% hexanes to 50% EtOAc and 2% formic acid in hexanes) to obtain **MN-455** (526 mg, 91%) as a yellow solid: mp 235-237 °C; ^{1}H NMR (400 MHz, DMSO-d_6) δ 12.69 (s, 1H), 11.31 (s, 1H), 7.91 – 7.85 (m, 2H), 7.83 – 7.76 (m, 2H), 7.59 (dd, *J* = 8.4, 2.2 Hz, 1H), 7.30 (d, *J* = 2.3 Hz, 1H), 7.27 (s, 4H), 6.94 (d, *J* = 8.3 Hz, 1H), 6.72 – 6.67 (m, 1H), 6.29 – 6.23 (m, 1H), 5.79 (s, 1H), 2.36 (s, 3H), 1.45 (s, 6H) (Supplementary Figure 9).^{13}C NMR (101 MHz, DMSO-d_6) δ 167.2, 151.9, 137.2, 136.6, 134.8, 134.6, 133.4, 131.2, 129.78, 129.75, 129.2, 128.2, 127.0, 126.0, 125.3, 123.2, 121.9, 121.7, 116.9, 109.6, 107.2, 75.7, 27.2, 20.8 (Supplementary Figure 9).

Sodium 4-(5-(2,2-Dimethyl-4-(p-tolyl)-2H-chromen-6-yl)-1H-pyrrol-2-yl)benzoate (YCT-529, compound 1). MN-455 (526 mg, 1.21 mmol, 1.0 equiv) was dissolved in THF (10 mL) and water (10 mL), followed by the addition of NaOH (72 mg, 1.81 mmol, 1.5 equiv). The reaction mixture was stirred at room temperature for 6 h, and the solvent was evaporated under reduced pressure to obtain a dry residue. The product was purified by precipitation in 5% water in dioxane solvent to obtain **YCT-529** (629 mg, 92%) as an off-white powder. m.p. could not be determined; compound degrades >190 °C. ^{1}H NMR (400 MHz, $CDCl_3$) δ 11.16 (s, 1H), 7.82 (d, *J* = 8.0 Hz, 2H), 7.59 (td, *J* = 5.1, 2.3 Hz, 3H), 7.28 (d, *J* = 5.3 Hz, 5H), 6.91 (d, *J* = 8.3 Hz, 1H), 6.50 (t, *J* = 2.9 Hz, 1H), 6.20 (d, *J* = 3.0 Hz, 1H), 5.77 (s, 1H), 2.36 (s, 3H), 1.45 (s, 6H) (Supplementary Figure 10). Purity 96% (Supplementary Figure 11).

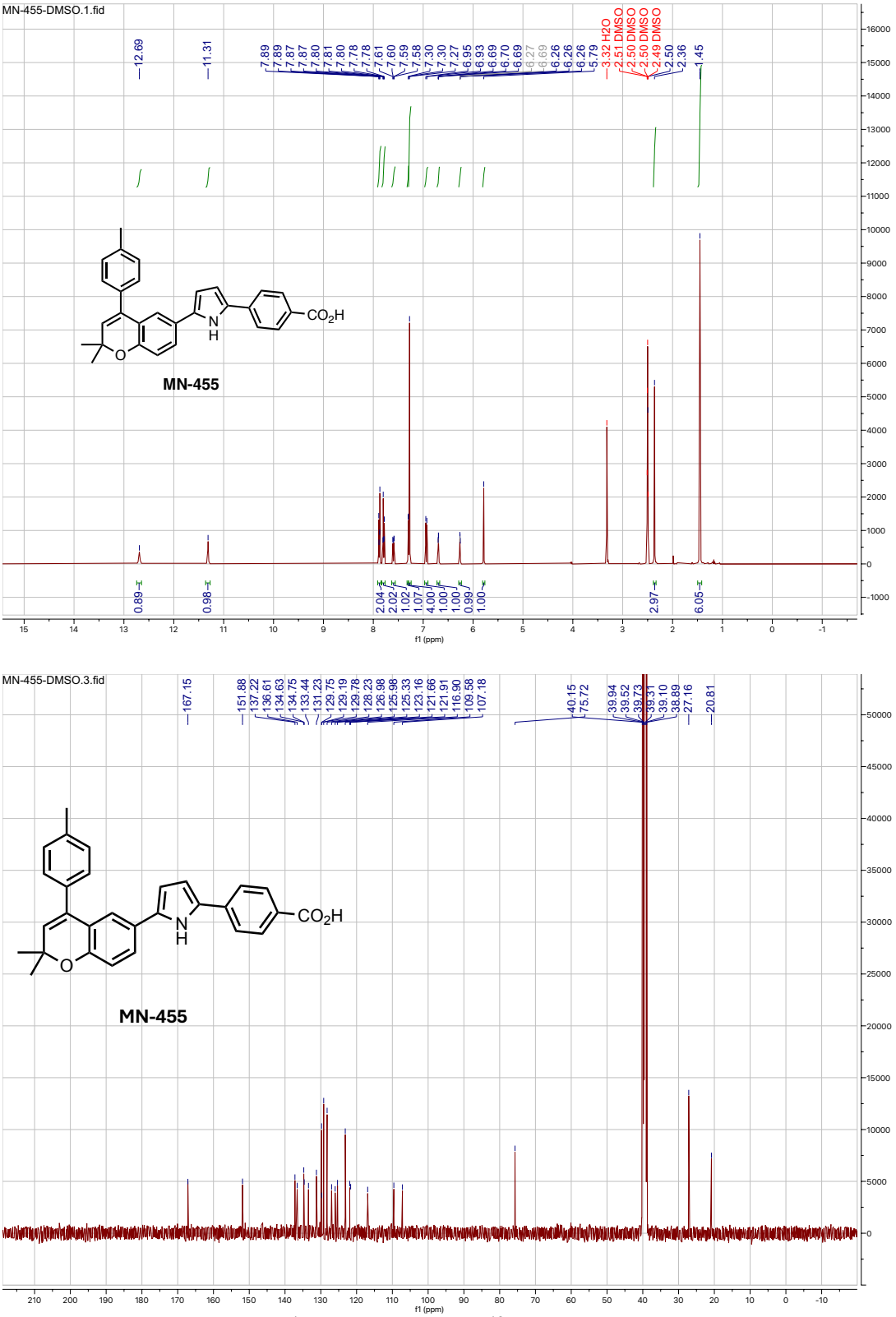

Supplementary Figure 9. ^{1}H NMR (top) and ^{13}C NMR (bottom) spectra for compound **MN-455**.

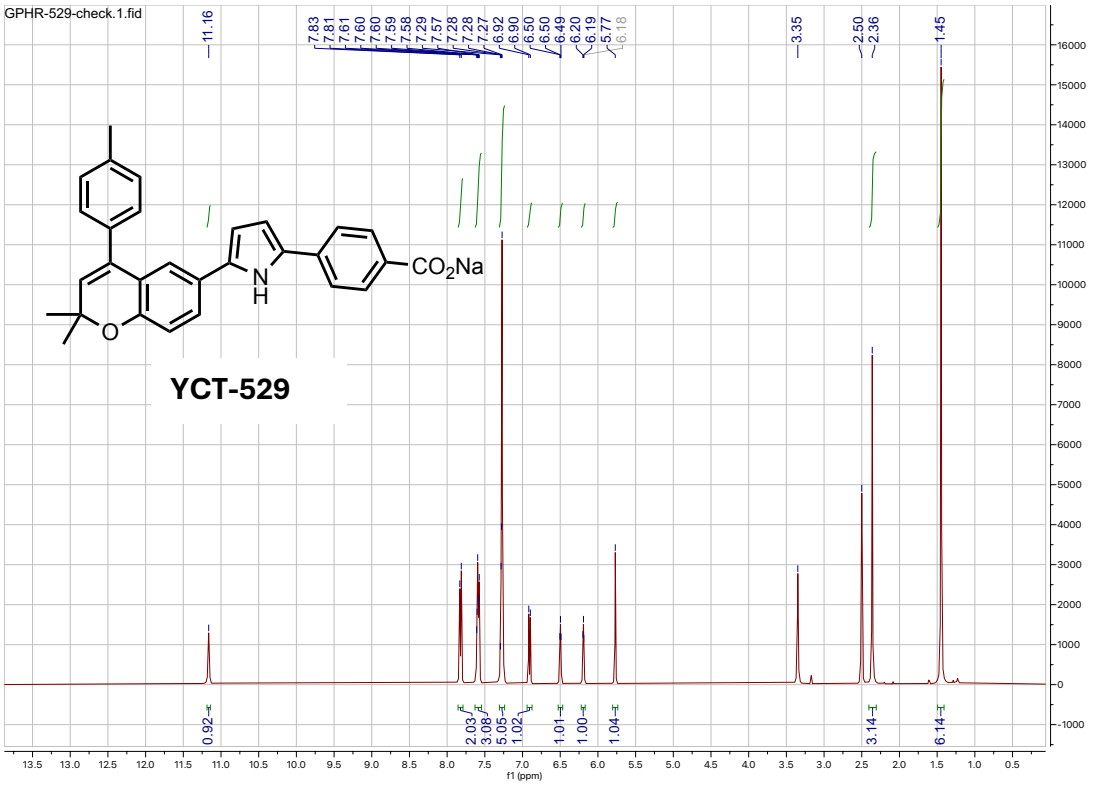

Supplementary Figure 10. ^{1}H NMR spectrum for **YCT-529**.

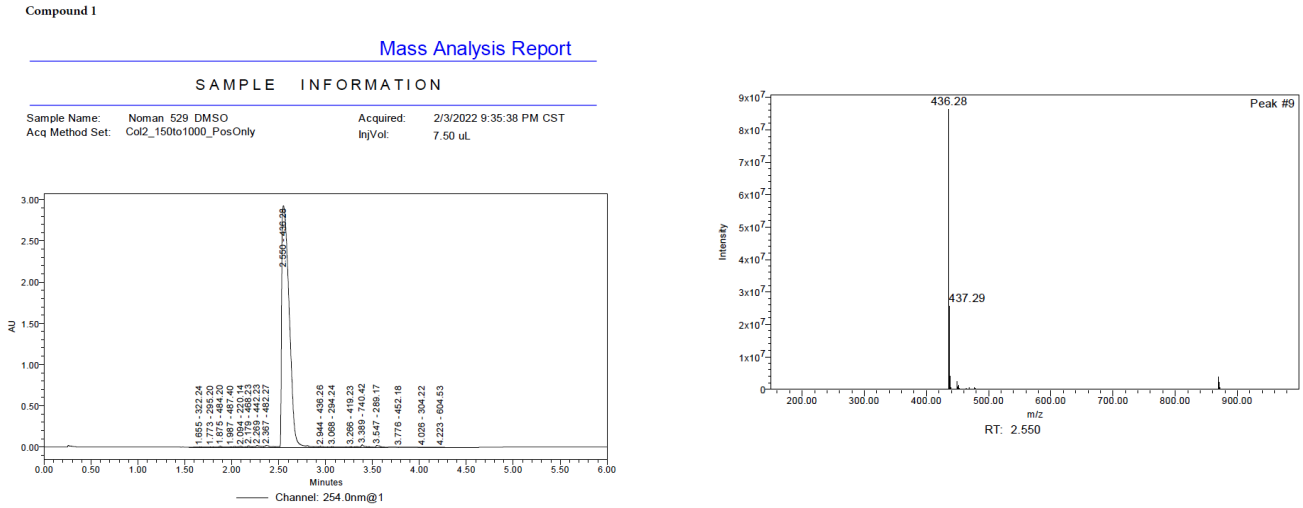

	RT	Area	% Area	Height	Base Peak (m/z)
1	1.655	2074	0.01	570	322.24
2	1.773	9162	0.05	3147	295.20
3	1.875	39291	0.23	10201	484.20
4	1.987	1039	0.01	1777	487.40
5	2.094	47682	0.28	10506	220.14
6	2.179	30659	0.18	16171	468.23
7	2.269	70271	0.42	22129	442.23
8	2.367	81470	0.48	20267	482.27
9	2.550	16202932	96.37	2926918	436.28
10	2.944	35921	0.21	9305	436.26
11	3.068	47868	0.28	7943	294.24
12	3.266	22813	0.14	7875	419.23
13	3.389	103676	0.62	28178	740.42
14	3.547	71762	0.43	25307	289.17
15	3.776	26859	0.16	2818	452.18
16	4.026	8303	0.05	980	304.22
17	4.223	11576	0.07	1497	604.53

Supplementary Figure 11. HPLC purity analysis for **YCT-529**.

References

1. Chung, S.S.*, et al.* Oral administration of a retinoic acid receptor antagonist reversibly inhibits spermatogenesis in mice. *Endocrinology* **152**, 2492-2502 (2011).
2. Chung, S.S.W.*, et al.* Pharmacological activity of retinoic acid receptor alpha-selective antagonists in vitro and in vivo. *ACS Med. Chem. Lett.* **4**, 446-450 (2013).
3. Chung, S.S., Wang, X. & Wolgemuth, D.J. Prolonged oral administration of a pan-retinoic acid receptor antagonist inhibits spermatogenesis in mice with a rapid recovery and changes in the expression of influx and efflux transporters. *Endocrinology* **157**, 1601-1612 (2016).
4. Russell, L.D., Ettlin, R.A., SinhaHikim, A.P. & Clegg, E.D. *Histological and histopathological evaluation of the testis*, (Cache River Press, Clearwater, FL, 1990).
5. Chung, S.S., Sung, W., Wang, X. & Wolgemuth, D.J. Retinoic acid receptor alpha is required for synchronization of spermatogenic cycles and its absence results in progressive breakdown of the spermatogenic process. *Dev. Dyn.* **230**, 754-766 (2004).
6. Chung, S.S., Wang, X. & Wolgemuth, D.J. Male sterility in mice lacking retinoic acid receptor alpha involves specific abnormalities in spermiogenesis. *Differentiation* **73**, 188-198 (2005).
7. Travis, A.J.*, et al.* Functional relationships between capacitation-dependent cell signaling and compartmentalized metabolic pathways in murine spermatozoa. *J. Biol. Chem.* **276**, 7630-7636 (2001).